

Structural Transformation of Fluorinated Carbon Nanotubes Induced by in Situ Electron-Beam Irradiation

Kay Hyeok An,[†] Kyung Ah Park,[†] Jeong Gu Heo,[†] Ji Yeong Lee,[‡] Kwan Ku Jeon,[†] Seong Chu Lim,[†] Cheol Woong Yang,[§] Young Seak Lee,^{||} and Young Hee Lee^{*†}

Contribution from the BK21 Physics Division, Institute of Basic Science, Department of Nanoscience and Technology, and Department of Advanced Materials Engineering, Center for Nanotubes and Nanostructured Composites (CNNC), Sungkyunkwan University, Suwon 440-746, Korea, and Department of Chemical Engineering, Nanotechnology Center, Sunchon National University, Sunchon 540-742, Korea

Received September 7, 2002; E-mail: leeyoung@yurim.skku.ac.kr

Abstract: We have investigated the structural transformation of fluorinated singlewalled nanotubes (SWNTs) induced by electron-beam irradiation during the transmission electron microscope observations. Heavily fluorinated SWNT bundles were systematically transformed into multiwall-like nanotubes by releasing fluorine atoms during electron-beam irradiation and even broken into two pieces of the capped graphitic structures. Such structural transformations at relatively low kinetic energy (≤ 300 keV) could be explained by the local strains induced by fluorination, where C–C bonds that were fluorine-attached became 1.53 Å, a single bond similar to that of a diamond, from our density functional calculations. We propose a possible concerted pathway for the structural transformation of fluorinated SWNTs induced by electron-beam irradiation based on the experimental observations.

I. Introduction

Chemical functionalization of the carbon nanotube sidewalls is a useful approach to (i) modify the electronic structures, (ii) possibly improve the wettability of nanotubes in various aqueous solutions by changing nanotubes from hydrophobic to hydrophilic, (iii) functionalize further for chemical and biological sensors, and (iv) increase the specific surface area of the nanotubes. For instance, functionalization of carbon nanotubes by atomic hydrogen could modify the electronic structures from metallic to semiconducting without significant damage on the tube wall, although enhancement of wettability is not expected due to small charge transfer between carbon and hydrogen atoms.^{1,2} On the other hand, functionalization of carbon nanotubes by fluorine gas decreases the conductivity with increasing doping content, and the wettability improves, remarkably, which is of technological importance. However, the nanotube walls are disintegrated at high doping content, which limits their applications.^{3–5} Therefore, a precise control of chemical functionalization and understanding of the related structural modification are the key ingredients prior to the real applications.

Unless singlewalled carbon nanotubes (SWNTs) are seriously defective, they are generally stable to an electron-beam irradiation with an ordinary kinetic energy of up to 300 keV for a short irradiation time in high-resolution transmission electron microscope (HRTEM) observations. Even though the neighboring SWNTs were found to have coalesced into those with a larger diameter at a high temperature of 800 °C in HRTEM with an electron kinetic energy of 1.25 MeV, such a coalescence could still be explained by the generation of various defects on the tube walls.⁶ However, the electron irradiation of SWNTs at a relatively low energy of 100 keV for 80 min in HRTEM could also distort a sidewall of isolated SWNT. Furthermore, it has been observed that higher irradiation with 200 keV for 26 min changed the bundle structure of SWNTs to an amorphous-like structure.⁷ This suggests that the total dose of electrons bombarding on the tube walls is an important factor in determining the stability of the tubes.

In this report, we have done a systematic study on the structural transformation of fluorinated SWNTs induced by in situ electron-beam irradiation during HRTEM observations. The unfluorinated SWNTs bundles with an individual SWNT-diameter of 1.5 nm are clearly observed, which is in good agreement with the value estimated from the Raman breathing. No structural deformation is observed from our unfluorinated samples in the electron energy up to 300 keV during the

[†] BK21 Physics Division, CNNC, Sungkyunkwan University.

[‡] Department of Nanoscience and Technology, CNNC, Sungkyunkwan University.

[§] Department of Advanced Materials Engineering, CNNC, Sungkyunkwan University.

^{||} Sunchon National University.

(1) Lee, S. M.; An, K. H.; Lee, Y. H.; Seifert, G.; Frauenheim, T. *J. Am. Chem. Soc.* **2001**, *123*, 5059–5063.

(2) Kim, K. S.; Bae, D. J.; Kim, J. R.; Park, K. A.; Lim, S. C.; Kim, J.-J.; Choi, W. B.; Park, C. Y.; Lee, Y. H. *Adv. Mater.* **2002**, *14*, 1818–1821.

(3) An, K. H.; Heo, J. G.; Jeon, K. K.; Bae, D. J.; Yang, C. W.; Park, C. Y.; Lee, Y. H. *Appl. Phys. Lett.* **2002**, *80*, 4235–4237.

(4) Mickelson, E. T.; Huffman, C. B.; Rinzler, A. G.; Smalley, R. E.; Hauge, R. H.; Margrave, J. L. *Chem. Phys. Lett.* **1998**, *296*, 188–194.

(5) Mickelson, E. T.; Chiang, I. W.; Zimmerman, J. L.; Boul, P. J.; Lozano, J.; Liu, J.; Smalley, R. E.; Hauge, R. H.; Margrave, J. L. *J. Phys. Chem. B* **1999**, *103*, 4318–4322.

(6) Terrones, M.; Terrones, H.; Banhart, F.; Charlier, J.-C.; Ajayan, P. M. *Science* **2000**, *288*, 1226–1229.

(7) Smith, B. W.; Luzzi, D. E. *J. Appl. Phys.* **2001**, *90*, 3509–3515.

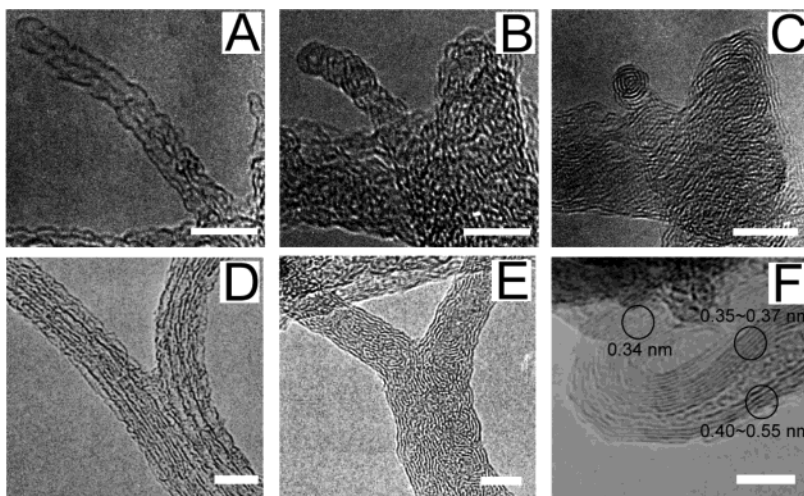


Figure 1. Time evolution of the TEM images for various phases: (A) the protruded F-SWNT bundle from the sample prepared at 300 °C before extensive irradiation; (B, C) the formation of the MWNT ring fringe after electron-beam irradiation of doses of $\sim 1.1 \times 10^{22}$ and $\sim 2.0 \times 10^{22}$ electrons cm^{-2} , respectively; the MWNT-like fringes were also shown in the background; (D) a Y-type fluorinated SWNT bundle prepared at a reaction temperature of 250 °C before extensive irradiation; (E) the Y-type bundle was transformed into the multiwall-like phase after irradiation of a dose of $\sim 2.1 \times 10^{22}$ electrons cm^{-2} ; and (F) several layered structures of the fluorinated SWNTs prepared at a reaction temperature of 300 °C coexist as intermediate phases with different separation distances indicated in the figure. The scale bar is 5 nm.

HRTEM observations. However, these bundles are rapidly transformed into multiwall-like phases from the samples fluorinated at 200 and 300 °C, which is never observed from the unfluorinated nanotubes. These structural transformations are explained in terms of the strains accumulated during fluorine release induced by electron-beam irradiation, which is supported by the density functional calculations.

II. Experimental Section

Preparation of SWNTs Powder. SWNTs powder was prepared by conventional catalytic arc discharge. The chamber was pumped down to a base pressure of 100 mTorr, and then helium gas was introduced to a pressure of 100 Torr. The total amount of catalysts (with the ratio of Ni:Co:FeS is 1:1:1) in a graphite powder was fixed at 5 wt %, where sulfur was added as a promoter. This significantly increased the yield of CNTs deposited in the chamber. The powder was collected from the chamber, collar, and cathode and then grinded together. The powder contained about 30 wt % of SWNTs and 8 wt % of transition metals. The details have been described elsewhere.⁸

Fluorination of SWNTs. The generated powder was brought into a Ni boat of the fluorine reaction chamber made by Ni and stainless steel 316 SS (17Cr – 12Ni – 2.5Mo) to prevent erosion. The chamber was pumped down to 10^{-2} Torr and purged by nitrogen gases to remove the residual oxygen and moisture. F_2 gas was then introduced into the chamber, with the pressure maintained at 0.2 bar for 10 min for a given reaction temperature. After the reaction, the chamber was again evacuated down to 10^{-2} Torr, and nitrogen gas was refilled prior to the extraction of the powder sample. Fluorine content increased up to 0.5 F/C at a reaction temperature of 300 °C.³ This composition was similar to the previously reported values.^{5,9} SWNTs fluorinated at a reaction temperature of up to 200 °C showed the ionic-bond characteristics, which implies the sidewall functionalization, whereas at a higher reaction temperature beyond 200 °C, they revealed the covalent-bond characteristics of CF_n ,³ implying that the tube structures are transformed into other phases. What is more fascinating is that the structural transformation of the fluorinated SWNTs took place in situ during electron-beam irradiation at a relatively low dose and low kinetic energy.

HRTEM Observation of Fluorinated SWNTs. The fluorinated SWNT powder was placed on a holey carbon micro-grid for the HRTEM observations. The structural transformation of SWNTs was observed

in a thermionic emission JEOL 3011 high-resolution TEM (300 keV, LaB₆) and a field emission JEOL 2010F high-resolution TEM (200 keV) at room temperature. An electron flux for each irradiation was estimated by calibrating the current density measured on the viewing screen. The changes in structure were recorded on a videotape during electron-beam irradiation. This videotape is available on our website: <http://nanotube.skku.ac.kr/>.

Theoretical Calculations of Fluorinated SWNTs. We used a self-consistent charge-density-functional-based tight-binding (SCC-DFTB) method to determine the most stable geometries of fluorinated nanotubes at different coverages. The SCC-DFTB method uses a basis of numerically described s and p atomic orbitals for carbon and fluorine atoms. Hamiltonian overlap matrix elements are evaluated by a two-center approach. Charge transfer is taken into account through the incorporation of a self-consistency scheme for Mulliken charges based on the second-order expansion of the Kohn–Sham energy in terms of charge density fluctuations. The diagonal elements of the Hamiltonian matrix employed are then modified by the charge-dependent contributions to describe the change in the atomic potentials due to the charge transfer. The off-diagonal elements have additional charge-dependent terms due to the Coulomb potential of ions. They decay as $1/r$ and thus account for the Madelung energy of the system. Further details of the SCC-DFTB method have been published elsewhere.¹⁰ A supercell of eight layers along the tube axis with (5,5) nanotube was used in the calculation. The total energy was calculated at the γ point with a periodic boundary condition along the tube axis.

III. Results and Discussion

Figure 1 shows a time evolution of the morphological changes of the SWNT bundle fluorinated at 300 °C, which corresponds to a coverage of F/C = 0.5,³ during the electron-beam irradiation with a kinetic energy of 300 keV (an electron flux of about 1.54×10^{19} electrons $\text{cm}^{-2} \text{s}^{-1}$). The original bundle with a diameter of about 40 Å was heavily distorted particularly in the middle due to the topological presence of fluorine atoms

- (8) Park, Y. S.; Kim, K. S.; Jeong, H. J.; Kim, W. S.; Moon, J. M.; An, K. H.; Bae, D. J.; Park, G. S.; Lee, Y. H. *Synth. Met.* **2002**, *126*, 245–251.
 (9) Kudin, K. N.; Bettinger, H. F.; Scuseria, G. E. *Phys. Rev. B* **2001**, *63*, 045413-1–045413-4.
 (10) Elstner, M.; Porezag, D.; Jungnickel, G.; Elsner, J.; Haugk, M.; Frauenheim, T.; Suhai, S.; Geifert, G. *Phys. Rev. B* **1998**, *58*, 7260–7268.

(Figure 1A). The SWNT walls of the fluorinated nanotubes were heavily distorted, and this could be explained by the strain developed upon fluorine adsorption, which will be discussed later. The electron-beam irradiation accumulates heavier strain on the tube walls, by presumably exiling fluorine atoms and thus accumulating the local strain in the adjacent tube bonds. The structural transformation in Figure 1B occurred within 12 min, corresponding to a dose of $\sim 1.1 \times 10^{22}$ electrons cm^{-2} . The electron-beam irradiation again highly excited fluorine atoms to exile from the tube wall, accumulating the local strain in the adjacent tube bonds. The electron-beam irradiation finally bent the bundle, which enabled us to observe the top view of the transformed structure, that is, a multiwall-like ring fringe (Figure 1C). We also note that the multiwall-like backbone images are clearly seen in Figure 1C. We should emphasize that this structural transformation was never observed from the unfluorinated sample within our typical observation time. The multiwall-like fringe is definitely different from the onion-like structure and may be formed from the interference of the bent tubes. This is in good contrast with the previous report on the pristine sample with an electron irradiation at 100 and 200 keV to a dose of $\sim 10^{23}$ electrons cm^{-2} , which is attributed to the knock-on damage to the top and bottom of the tube.⁷ Recent TEM results demonstrated that two SWNTs in the bundle were merged into the single SWNT with a larger diameter under illumination of the electron kinetic energy of 1.25 MeV at 800 °C, which was interpreted by the presence of the local defects on the tube wall.⁶ In our case, however, fluorine excitation by the electron beam (fluorine atoms have a larger cross section than do carbon atoms to the electron beam) created many defects locally on the tube walls, and the tube walls are merged into several layers, as shown in Figure 1C. These structural changes were further developed, until they completely formed layered structures.

It is also interesting to note the structural transformation from a Y-shape SWNT bundle to a multiwall-like layered phase (Figure 1D, E). In this case, the tubes in the bundle were defined better and less defective than the previous ones due to the low reaction temperature (250 °C). The time evolution of the structural transformation was rather slow. The multiwall-like phase kept changing during irradiation. We note that the outer parts of bundle start forming graphitic layers faster than do the inner ones. Similar phenomena were observed from many other different bundles. This implies an early exile of fluorine atoms from the outer walls, stabilizing the outer tube walls faster. In the sample prepared at 300 °C, the SWNT bundles were mostly transformed into multiwall-like layered phases (Figure 1F). It shows a typical layered phase with different layer distances, which was attributed to the nonuniformly distributed F-content in different regions. The layers that are 0.34 nm apart are close to the graphitic layers. Such a phase revealed a structural evolution no longer. This is again strong evidence that the fluorine atom plays an important role in structural transformation observed during electron-beam irradiation.

The structural transformation upon different fluorine composition can be clearly seen from the Raman spectroscopy, as shown in Figure 2. All of the samples have the maximum peak intensity near 1593 cm^{-1} , the so-called tangential mode, which is related to the graphite E_{2g} symmetric intralayer mode, split due to the curvature of the rolled-up graphene sheet. Two

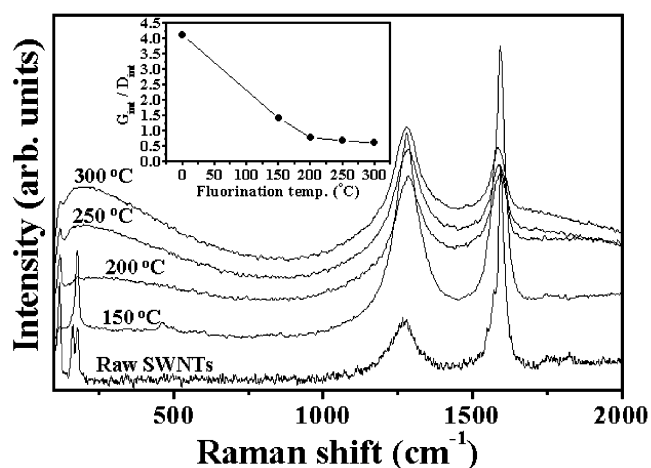


Figure 2. FT-Raman spectra of the fluorinated SWNTs as a function of fluorination temperatures.

shoulder peaks also appear at 1571 and 1552 cm^{-1} , which is a characteristic of SWNTs. A broad band is usually observed around 1280 cm^{-1} in graphite and MWNTs, which is a characteristic of amorphous carbon or defects, and is also observed in Figure 2. As the fluorination temperature increases, the intensity of the maximum peak at 1280 cm^{-1} increases drastically, whereas the intensity ratio of the 1593 to 1280 cm^{-1} peak decreases (inset), indicating some structural deformation in the tube wall after fluorination. The radial breathing modes (RBM) whose frequencies depend on the tube diameters in the low-frequency range of 100–200 cm^{-1} are also observed. This is also a characteristic of SWNTs, because MWNTs do not show any low-frequency mode. After fluorination, the RBM is retained up to 150 °C and disappears at 200 °C, indicating the structural changes of SWNTs. The heavy fluorination at high temperature could destroy the tube walls severely. However, because the two shoulder peaks at 1571 and 1552 cm^{-1} are present, the graphitically layered structures are still retained. The SWNTs are still maintained in the sample even at high temperature due to the presence of the RBM at 120 cm^{-1} .

To understand such a topological change, we show here the fluorine-decorated SWNT for different fluorine coverages (Figure 3). At low coverages of 0.2 and 0.3, fluorine atoms are chemisorbed and stable at some selective sites despite large lattice distortions. We have tried various types of fluorine decorations. Only those with high symmetry shown in Figure 3 were stable, and others were dissociated exothermally. This suggests that a topological attack by fluorine atoms may easily disintegrate the tube wall. The binding energy is calculated after full geometrical optimization by the conjugate gradient method, where $E_b(\text{C-F}) = E_t(\text{C-F}) - E_t(\text{C}) - N_f E_{\text{self}}(\text{F})$. Here E_t is the total energy of the system, and N_f and $E_{\text{self}}(\text{F})$ are the number of fluorine atoms and its atomic energy, respectively. At high coverage ($F/C = 0.5$), fluorine atoms are chemisorbed with a large binding energy of -5.44 eV with a bond length of 1.35 Å (CF_4), but again induce a remarkable lattice distortion in the C–C bonds with an average strain energy of 0.8 eV per fluorine atom. Some bond lengths are extended to that of a single bond, 1.55 Å, which is similar to that of diamond. This was attributed to the Mulliken charge transfer (0.19 e) to the fluorine atoms. It implies that this bond energy was reduced at least by 25%; that is, three single bonds instead of four single bonds in diamond were formed in the tube wall. In addition to the present

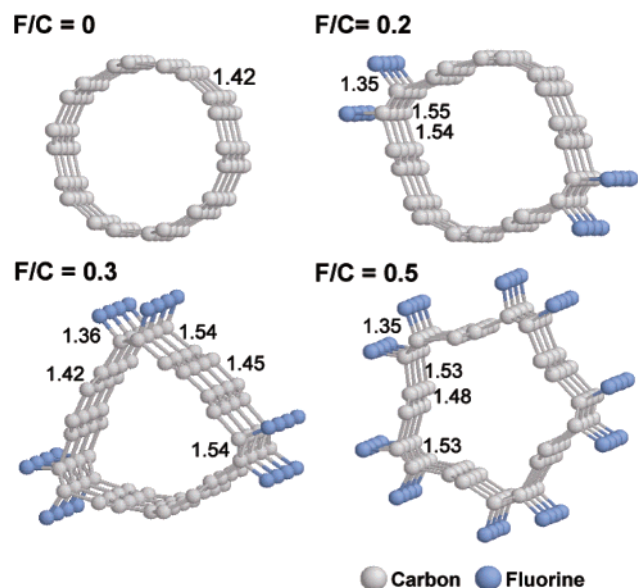


Figure 3. Ball-and-stick fluorinated SWNT at different coverage predicted by the density functional calculations. A supercell of eight layers along the tube axis with (5,5) nanotube was used in the calculation. The total energy was calculated self-consistently at the γ point with a periodic boundary condition along the tube axis. This evaluated the amount of charge transfer accurately from carbon atoms to fluorine atoms. The C–C back-bonds near fluorine atoms were extended to a single bond, which can be attributed to the Mulliken charge transfer (0.19 e) to the fluorine atoms. The bond lengths are in units of Å.

stripe type shown in Figure 3, some isomers could also exist with relatively weaker binding energies.⁹ It is well known that fluorine atoms are more susceptible to the irradiated electron beam due to a larger cross-sectional area as compared to that of carbon atoms. Therefore, fluorine atoms can be thermally excited more easily than carbon atoms and thus topologically exiled easily from the tube wall, transferring an extra strain on the host tube walls, and at the same time the separation distance of the tube walls is shortened. This increases the probability of the tubes to be broken into small pieces, similar to Figure 1C. Once the bundle is cut into two pieces, the tube ends will be capped further to stabilize the edge energy, where the activation barrier height could be easily overcome by the continuously supplied electron-beam energy.

Figure 4 shows a time evolution of the morphological changes of the SWNT bundle fluorinated at 250 °C during the condensed electron-beam irradiation at an electron flux of about 1.7×10^{22} electrons $\text{cm}^{-2} \text{s}^{-1}$ with a kinetic energy of 200 keV. Despite the relatively low kinetic energy of the electron beam (200 keV FE-gun, JEM-2010F), we observed that the SWNT bundle was chopped into two pieces of the capped multiwalled carbon nanotubes (MWNTs) (Figure 4). The fluorinated SWNT bundle seems to be very defective, unlike the pristine sample, as shown in Figure 4A. The separation distances between the tube walls are irregular along the tubes, indicating that fluorine atoms are not uniformly distributed over the bundle. This bundle was transformed to a phase that is more likely amorphous in nature during the electron-beam irradiation (Figure 4B). Graphitically layered structures start forming locally (Figure 4C). The defective parts, which are not yet graphitized, may accumulate heavy strains. Such a local area under heavy strains can easily be disintegrated with further irradiation of the electron beam, resulting in the separation of two MWNTs (Figure 4D).

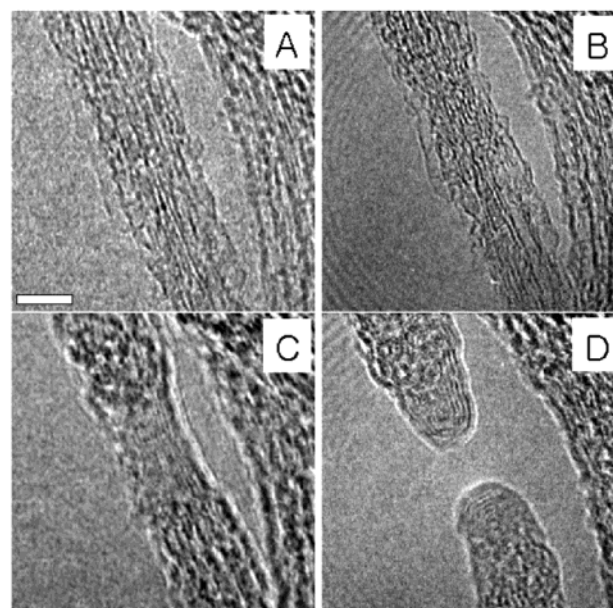


Figure 4. Time evolution of the morphological changes of the SWNT bundle fluorinated at 250 °C during the condensed electron-beam irradiation at an electron flux of about 1.7×10^{22} electrons $\text{cm}^{-2} \text{s}^{-1}$ with a kinetic energy of 200 keV. No extra heating was applied to the sample. It took several tens of seconds for the SWNT bundle to be chopped into two pieces. The scale bar is 5 nm.

We illustrate schematically a concerted pathway of the structural transformation induced by the electron-beam irradiation as follows (Figure 5). The bundle structure of the fluorinated SWNTs is shown in Figure 5A. The local strain can be accumulated in the tube wall of the bundle due to desorption of fluorine atoms triggered by the electron-beam irradiation. This may enhance coalescence of SWNTs to those with larger diameter (Figure 5B), which was observed in TEM with high kinetic energy.⁶ At the same time, the length of the bundle may get shorter, similar to Figure 3. The next step is the fragmentation of the graphitic shells in the tubes into small pieces induced again by the local strain due to desorption of fluorine atoms and the accumulated thermal energy from the electron-beam irradiation (Figure 5C). The fragmented graphitic shells will coalesce to MWNTs to minimize the edge energy (Figure 5D). The extra energy gain is accomplished by van der Waals interactions between the tube walls. At the same time, the tubes can also be capped. When the edge-on (or capped) parts are overheated by the electron-beam irradiation, this again gives rise to a collapse of the capped edges.¹¹ This process is therefore similar to the cap opening by thermal annealing process,^{12,13} but induced by the strain accumulated with fluorine atoms and electron-beam energy in our case. Because significant strain energy (0.05 eV/atom) is accumulated in the tube,¹⁴ there is a chance for those sheets to be flattened to form graphitic layers (Figure 5E). This should occur, when the graphitic sheet is large enough such that the energy gain by the strain release exceeds the energy cost of the edge.

(11) Crespi, V. H.; Chopra, N. S.; Cohen, M. L.; Zettl, A.; Radmilovic, V. *Appl. Phys. Lett.* **1998**, *73*, 2435–2437.

(12) Liu, J.; Rinzler, A. G.; Dai, H.; Hafner, J. H.; Bradley, R. K.; Boul, P. J.; Lu, A.; Iverson, T.; Shelimov, K.; Huffman, C. B.; Rodriguez-Macias, F.; Shon, Y. S.; Lee, T. R.; Colbert, D. T.; Smalley, R. E. *Science* **1998**, *280*, 1253–1256.

(13) Pompeo, F.; Resasco, D. E. *Nano Lett.* **2002**, *2*, 369–373.

(14) Oh, D. H.; Lee, Y. H. *Phys. Rev. B* **1998**, *58*, 7407–7411.

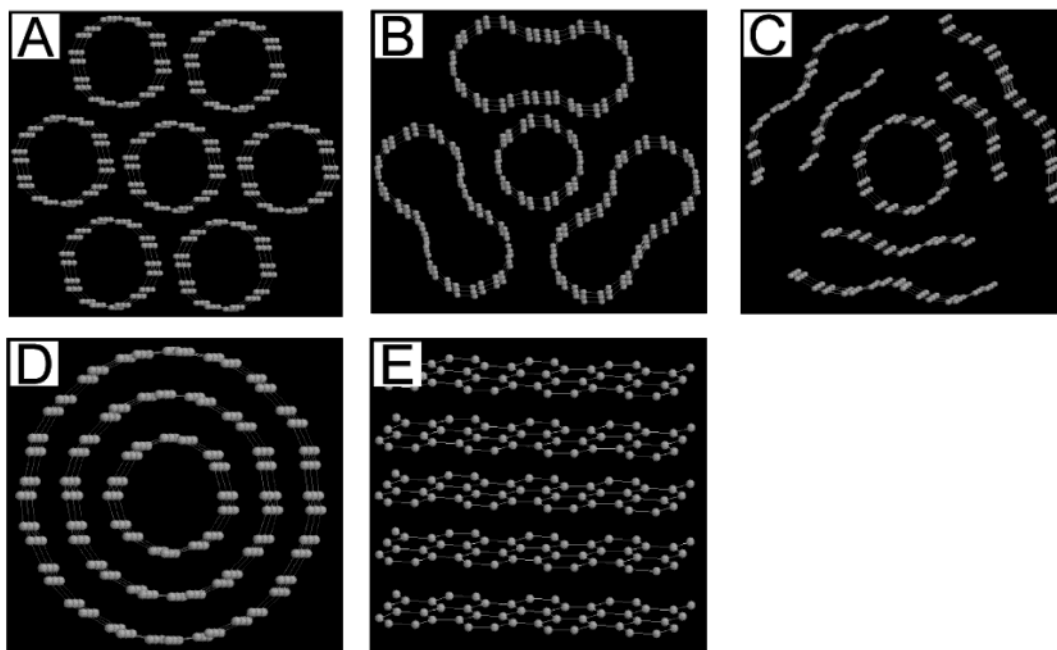


Figure 5. Schematic diagram of electron-beam-induced structural transformation of F-doped SWNTs: (A) ideal SWNT bundle, (B) coalescence of SWNTs into those with larger diameter, and (C) partial fragmentation of the SWNT wall induced by the local strain. The graphitic flake can be recombined to form either (D), multiwalled CNT, or (E), complete graphitic layers.

The structural transformation strongly depends on the reaction temperature, that is, the doping content. The Coulomb repulsion between charged fluorine atoms keeps the doping content less than 0.5. One important practical aspect of the fluorinated SWNTs is the significant enhancement of the wettability in water. The fluorinated SWNTs were completely dispersed without aggregation for several months, unlike the pristine SWNTs in water, which easily aggregate. This property is important in energy storage particularly in improving the capacitance of the supercapacitor and nanocomposites with various organic solutions as well. Another important property of the fluorinated SWNTs is the modification of the electronic structures, where the conductivity of the SWNTs mat was reduced with increasing fluorination content.³ The band structure of F-decorated SWNT at a coverage of 0.5 clearly showed that the metallic tube was transformed into the semiconducting tube.¹⁵ A precise control of the F-content may lead to a new possibility for applying this material to various disciplines.

(15) Park, K. A.; Lee, Y. H., unpublished results.

Conclusions

We have reported various phase transformations of the fluorinated SWNTs induced by electron-beam irradiation during the HRTEM observations at relatively low kinetic energy (300 keV). Our density functional calculations suggested that a heavy strain on the C–C bonds in the tube wall was attributed to decoration of the tube wall by fluorination. Because fluorine atoms were more susceptible than carbon atoms to the electron-beam irradiation, fluorine atoms can be easily desorbed. This accumulates more strain on the host tube wall, eventually leading to various structural transformations. We proposed a possible concerted pathway for the structural transformation of the fluorinated SWNTs induced by electron-beam irradiation based on the experimental observations. Precise structure control of SWNTs by fluorine composition should be done prior to applications for efficient energy storage and nanocomposites.

Acknowledgment. This work was supported by the MOST through the NRL program and in part by CNNC at SKKU.

JA028453M